Dyes and Pigments 83 (2009) 102–110

Contents lists available at ScienceDirect

Dyes and Pigments

journal homepage: www.elsevier.com/locate/dyepig

Novel luminescent polymers containing backbone triphenylamine groups and pendant quinoxaline groups

Wei Shi [a], Lei Wang [b], Hongyu Zhen [c], Dexi Zhu [c], Tunsagul Awut [a], Hongyu Mi [a], Ismayil Nurulla [a,*]

[a] Key Laboratory of Petroleum and Gas Fine Chemicals, Educational Ministry of China, School of Chemistry and Chemical Engineering, Xinjiang University, Urumqi 830046, PR China
[b] Institute of Polymer Optoelectronic Materials and Device, Key Lab of Specially Functional Materials of the Ministry of Education, South China University of Technology, Guangzhou 510640, PR China
[c] State Key Laboratory of Modern Optical Instrumentation, Zhejiang University, Hangzhou 310027, PR China

ARTICLE INFO

Article history:
Received 31 January 2009
Received in revised form
20 March 2009
Accepted 23 March 2009
Available online 5 April 2009

Keywords:
Triphenylamine
Quinoxaline
Polyfluorene
Backbone
Pendant
Electroluminescence

ABSTRACT

Novel, conjugated polyfluorene derivatives that comprised an electron-donating triphenylamine group in the backbone and pendant, electron-accepting quinoxaline moieties, were synthesized via the Suzuki coupling reaction and their UV–vis absorption, fluorescence emission and electrochemical properties were investigated. The copolymers were readily soluble in common organic solvents and displayed good film-forming ability and excellent thermal stability. Electroluminescence devices, comprising indium tin oxide/poly(3,4-ethylenedioxythiophene) doped with poly(styrenesulfonic acid)/emitting polymer/Ba/Al, in which the polymers were employed as emissive layers, exhibited superior performance compared to that of corresponding, poly(9,9-dioctylfluorene) and poly(9,9-dioctylfluorene-*co*-4,4′-triphenylamine) based devices, indicating that the polymers offer promise as emissive materials in polymeric light-emitting diodes.

1. Introduction

Light-emitting diodes based on conjugated polymers (PLEDs) have attracted extensive attention in recent years due to their promising perspectives in the next generation of full-color flat panel displays [1–15]. One of the many important challenges that still remain is the improvement of the external quantum efficiency (EQE) of PLEDs. Generally, a PLED is a thin-film multilayer structure consists of a hole-transporting, an emitting, and an electron-transporting layer sandwiched between two electrodes. Charge carriers (holes and electrons) are injected separately from anode and cathode, recombine in the emitting layer and thus emit light [16]. Balanced rates of injection and transport for both carriers are essential to achieve high EQE in a PLED. A straightforward approach to improve the EQE of a PLED is to integrate the functions of carriers' transport and light emission into a single polymer, thereby creating an ambipolar (donor/acceptor) emissive polymer [17–19]. However, for polymers with $(donor–acceptor)_n$ ($(D–A)_n$) type backbones, the rather strong intramolecular charge transfer (ICT) along the main chains is prone to decrease their emissive efficiency in spite of the enhancement of both carriers' transport [17–19]. An alternative strategy to overcome this problem is to prepare polymers with p-type backbones and n-type side chains [20]. Based on this consideration, a series of poly(phenylenevinylene) (PPV) derivatives with peripheral oxadiazole groups were successfully prepared and exhibited promising electroluminescent properties [21–23]. But the application of these materials was restrained by the difficulties in their syntheses. The preparation of other types of polymers with p-type backbones and n-type side chains by relatively simpler synthesis is highly desirable.

Triarylamine (TAA) derivatives, small molecules [24–26] or polymers containing TAA units [27–31] are one type of the most widely used hole-transport materials because they are easily oxidized to form stable radical cations [32]. The incorporation of TAA segments into polymers can also improve their solubility and glass-formability. On the other hand, one type of n-building block, quinoxaline, was aroused special interest in recent years due to its high electron affinity and good thermal stability [33–35]. It has been successfully incorporated into polymers [36–38] to apply as the electron-transport materials in multilayer PLEDs. The attempts to simultaneously incorporate triphenylamine and quinoxaline into small molecules have been proven to be an effective way to obtain

* Corresponding author. Tel.: +86 0991 8583575; fax: +86 0991 8582809.
E-mail address: Ismayilnu@sohu.com (I. Nurulla).

0143-7208/$ – see front matter © 2009 Elsevier Ltd. All rights reserved.
doi:10.1016/j.dyepig.2009.03.016

materials with high luminescent efficiency [39–41]. But to our knowledge, the polymer with triphenylamine in backbone and quinoxaline as pendant has not been reported nowadays. The preparation of such polymers will be interesting to be explored. It's a potential protocol to integrate the good processibility and modified carriers' transport into a single polymer without compromising its luminescent efficiency.

This study reports the preparation and characterization of a series of polyfluorene derivatives with triphenylamine segment in polymers' backbones and quinoxaline group as pendant to polymer main chains. The photophysical, electrochemical and electroluminescence properties of these copolymers are systematically investigated here.

2. Experimental section

2.1. Materials

All manipulations involving air-sensitive reagents were performed under an atmosphere of dry nitrogen. All reagents, unless otherwise specified, were obtained from Aldrich, Acros, and TCI Chemical Co. and were used as received. Triethylamine (NEt_3), tetrahydrofuran (THF) and toluene were distilled from sodium at the presence of benzophenone and degassed before use. 2,7-Dibromo-9,9-dioctylfluorene (**5**) [42,43], and 2,7-bis(4,4,5,5-tetramethyl-1,3,2-dioxaborolan-2-yl)-9,9-dioctylfluorene (**6**) [42,43], were prepared according to the published procedures and have been described elsewhere.

2.2. Instrumentation

The ^{1}H NMR and ^{13}C NMR spectra were collected on a VARIAN INOVA-400 spectrometer operating respectively at 400 MHz (for ^{1}H) and 100 MHz (for ^{13}C) in deuterated chloroform solution with tetramethylsilane as reference. IR spectra were recorded on an EQUINOX 55 FT-IR spectrometer with KBr pellets. Elemental analyses were performed on a Vario EL Elemental Analysis Instrument (Elementar Co.). Number-average (M_n) and weight-average (M_w) molecular weights were determined by a Waters GPC 2410 in tetrahydrofuran (THF) using a calibration curve of polystyrene standards. UV–visible absorption spectra were recorded on an SHIMADZU UV-2450 UV–Vis spectrophotometer. PL spectra were recorded on HITACHIF-4500 spectrophotometer. Cyclic voltammetry was carried out on a CHI660C electrochemical workstation with platinum electrodes at scan rate of 50 mV/s against a saturated calomel electrode (SCE) with nitrogen-saturated solution of 0.1 M tetrabutylammonium hexafluorophosphate (Bu_4NPF_6) in acetonitrile (CH_3CN). Thermogravimetric and differential scanning calorimetric analyses (TGA and DSC) were conducted on NETZSCH STA 449C at a heating rate of 20 °C/min and 10 °C/min in nitrogen, respectively.

2.3. LED fabrication and characterization

Polymers were dissolved in toluene and filtered through a 0.45 μm filter. Patterned indium tin oxide (ITO) coated glass substrates were cleaned with acetone, detergent, distilled water and isopropanol, subsequently in an ultrasonic bath. After treatment with oxygen plasma, 50 nm of poly (3,4-ethylenedioxythiophene) (PEDOT) doped with poly(styrenesulfonic acid) (PSS) (Baytron-P 4083, Bayer AG) was spin-coated onto the substrate followed by drying in a vacuum oven at 80 °C for 8 h. A thin film of electroluminescent polymer was coated onto the anode by spin casting inside a dry box. The film thickness of the active layers was around 80 nm, as measured with a Tencor Alfa step 500 surface profiler (Oriel). Ba and Al layers were vacuum-evaporated on top of an EL polymers under a vacuum of 1×10^{-4} Pa. Device performances were measured inside a dry box. Current–voltage (I–V) characteristics were recorded with a Keithley 236 source meter. EL spectra were recorded by Oriel Instaspec IV CCD Spectrograph. Luminance and external quantum efficiencies were determined by a calibrated photodiode.

2.4. Synthesis of the monomers

2.4.1. Synthesis of N,N-bis(4-bromophenyl)aniline (*1*)

Toluene (110 mL), aniline (10.22 g, 109.7 mmol), 1-bromo-4-iodobenzene (69.8 g, 246.7 mmol), phenanthroline (0.74 g, 4.0 mmol), cuprous chloride (CuCl) (0.43 g, 4.0 mmol) and potassium hydroxide (KOH) (flakes, 86%, 58.9 g, 861.4 mmol) were added sequentially to a 500 mL three-necked flask equipped with condenser, mechanical stirrer, nitrogen inlet and outlet under nitrogen. The reaction mixture was heated to reflux in 30 min and was stirred at refluxing for 48 h. Then the mixture was cooled to 75 °C, and 150 mL of toluene and 100 mL of distilled water were used in extraction. The toluene phase was separated, dried with anhydrous magnesium sulfate ($MgSO_4$), filtered and vacuum distilled. The crude product was purified by silica column chromatography using petroleum ether as eluent to give **1** (26.0 g, 60%) as colorless viscous liquid. FT-IR (KBr, cm^{-1}): 3083, 3062, 3034, 1580, 1484, 1453, 1327, 1310, 1274 (C–N), 1172, 1104, 895, 826, 753, 706, 666. ^{1}H NMR ($CDCl_3$, ppm) δ: 7.36–7.34 (d, 4H), 7.30–7.26 (t, 2H), 7.09–7.07 (m, 3H), 6.96–6.94 (d, 4H). ^{13}C NMR ($CDCl_3$, ppm) δ: 146.86, 146.49, 132.30, 129.51, 125.37, 124.56, 123.70, 115.40.

2.4.2. Synthesis of N,N-bis(4-bromophenyl)-4′-iodophenylamine (*2*)

N,*N*-bis(4-bromophenyl)aniline (**1**) (2.02 g, 5.0 mmol), potassium iodide (0.83 g, 5.2 mmol), potassium iodate (1.6 g, 7.7 mmol) and acetic acid (15 mL) were added sequentially to a 50 mL two-necked round bottom flask equipped with condenser, magnetic stirrer, nitrogen inlet and outlet under nitrogen. The reaction mixture was stirred overnight at 80 °C under nitrogen. Then the mixture was cooled to room temperature and poured into 200 mL of water. The precipitate was collected and dissolved by CH_2Cl_2, washed with aqueous $Na_2S_2O_3$ and dried over anhydrous $MgSO_4$. After removing the solvent in vacuo, the residue was recrystallized from acetone to afford white solid (1.54 g, 61%). FT-IR (KBr, cm^{-1}): 3053, 1573, 1485, 1312, 1282, 1270 (C–N), 1173, 1103, 1071, 1003, 939, 818, 709, 666. ^{1}H NMR ($CDCl_3$, ppm) δ: 7.58–7.52 (d, 2H), 7.41–7.32 (d, 4H), 6.99–6.89 (d, 4H), 6.84–6.77 (d, 2H). ^{13}C NMR ($CDCl_3$, ppm) δ: 146.80, 145.98, 138.48, 132.59, 125.84, 125.79, 116.23, 86.40 (C–I).

2.4.3. Synthesis of N,N-bis(4-bromophenyl)-4′- (phenylethenyl) phenylamine (*3*)

To a 50 mL two-necked round bottom flask containing $Pd(PPh_3)_2Cl_2$ (65.8 mg, 0.094 mmol), CuI (18.9 mg, 0.189 mmol) and *N*,*N*-bis(4-bromophenyl)-4′-iodophenylamine (**2**) (1.0 g, 1.89 mmol) in triethylamine (NEt_3) (5.5 mL) and anhydrous THF (11 mL) was added phenylacetylene (197 mg, 1.89 mmol) under N_2. The reaction mixture was stirred at room temperature for 24 h. Then this mixture was filtered and the solvent was removed in vacuo. Silica gel column chromatography (petroleum ether: CH_2Cl_2 = 20:1, v/v) gave target product as white solid (0.70 g, 74%). FT-IR (KBr, cm^{-1}): 3059 (ar. C–H), 3033, 2215 (C≡C), 1581, 1507, 1483 (ar. C=C), 1314, 1286, 1267 (C–N), 1070, 1008, 822, 755, 689. ^{1}H NMR ($CDCl_3$, ppm) δ: 7.52–7.49 (m, 2H), 7.42–7.26 (m, 9H), 7.01–6.94 (dd, 6H). ^{13}C NMR ($CDCl_3$, ppm) δ: 146.89, 145.98, 132.84, 132.60, 131.55, 128.39, 128.17, 126.13, 123.40, 123.11, 117.55, 116.37, 89.24 ('C≡C), 89.22 (C≡C').

2.4.4. Synthesis of N,N-*bis(4-bromophenyl)-4′-(3-phenylquinoxaline) phenylamine (**4**)*

To a solution of *N*,*N*-bis(4-bromophenyl)-4′-(phenylethenyl)phenylamine (**3**) (1.4 g, 2.78 mmol) in CH_2Cl_2 (15 mL), $KMnO_4$ (1.4 g, 8.76 mmol), $NaHCO_3$ (0.284 g, 3.38 mmol) and tetraethylammonium bromide (0.284 g) were added by dissolving in water (15 mL). The mixture was vigorously stirred at room temperature for 48 h. The excess $KMnO_4$ was destroyed by addition of HCl and Na_2SO_3 until the red color disappeared. The organic layer was separated, washed with sodium dicarbonate and water, and dried by $MgSO_4$. After removal of the solvent, the residue was refluxed with 1,2-phenylenediamine (0.321 g, 2.92 mmol) in 50 mL of acetic acid under nitrogen atmosphere overnight. The reaction mixture was cooled to room temperature and poured into a large amount of cold water. The yellow precipitate was filtered and washed several times by hot water. The crude product was purified by column chromatography (silica gel, petroleum ether: CH_2Cl_2 = 1:1, v/v) to afford the target compound as bright yellow solid (1.2 g, 71%). FT-IR (KBr, cm^{-1}): 3054(ar. C–H), 1604, 1577, 1536 (C=N), 1509, 1484 (ar. C=C), 1314, 1270 (C–N), 1070, 1005, 818, 755, 714, 694. ^{1}H NMR ($CDCl_3$, ppm) δ: 8.19–8.17 (m, 2H), 7.79–7.76 (m, 2H), 7.57–7.55 (m, 2H), 7.42–7.36 (m, 9H), 6.99–6.95 (m, 6H). ^{13}C NMR ($CDCl_3$, ppm) δ: 153.48 (C=N), 152.75 (C′ = N), 147.55, 146.00, 141.23, 141.13, 139.24, 133.44, 132.52, 131.18, 130.07, 129.88, 129.79, 129.23, 129.08, 128.97, 128.31, 126.11, 122.89, 116.28. ($C_{32}H_{21}Br_2N_3$) (607): Calcd. C 63.28, H 3.49, N 6.92; Found C 63.17, H 3.52, N 6.85.

2.5. Synthesis of the polymers

The following general procedure [44] was used for the preparation of all the copolymers and reference polymers (poly (9,9-dioctylfluorene) (PFO) and poly(9,9-dioctylfluorene-*co*-4,4′-triphenylamine) (PFTPA)). To a three-necked flask were added 2,7-bis(4,4,5,5-tetramethyl-1,3,2-dioxaborolan-2-yl)-9,9-dioctylfluorene (**6**) (321 mg, 0.5 mmol), 2,7-dibromofluorene (**5**) and *N*,*N*-bis(4-bromophenyl)-4′-(3-phenylquinoxaline) phenylamine (**4**) (total 0.5 mmol), palladium acetate ($Pd(OAc)_2$) (3 mg) and tris(cyclohexyl)phosphine (6 mg). Then 8 mL of degassed toluene and 2 mL of tetraethylammonium hydroxide (Et_4NOH, 20% aqueous solution) were added via syringe. The reaction mixture was bubbled with N_2 for 30 min and stirred at refluxing for 3 days, then was poured into 200 mL of methanol. The resulted precipitate was recovered by filtration, purified by silica column chromatography with toluene as eluent to remove small molecules complex and catalyst residue. The pure copolymers were obtained after drying under vacuum at 50 °C overnight.

2.5.1. PFTQ-50 copolymer

FT-IR (KBr, cm^{-1}): 3059, 3032 (ar. C–H), 2926, 2854 (alky. C–H), 1598, 1510 (C=N), 1465, 1396, 1343, 1319, 1291, 1222, 1184, 1056, 977, 814, 760, 696. ^{1}H NMR ($CDCl_3$, ppm) δ: 8.23–8.18 (m, 2H), 7.79–7.77 (m, 4H), 7.64–7.58 (m, 10H), 7.48–7.42 (m, 5H), 7.29–7.26 (m, 4H), 7.16–7.14 (d, 2H) 2.06 (br, 4H, fluorene, C-9, $-CH_2-$), 1.26–1.08 (m, 20H), 0.82 (m, 10H). ^{13}C NMR ($CDCl_3$, ppm) δ: 153.53 (C=N), 153.00 (C′ = N), 151.70, 148.21, 146.27, 141.28, 141.07, 139.90, 139.40, 139.24, 136.68, 132.60, 132.52, 131.03, 129.98, 129.80, 129.19, 129.05, 128.90, 128.33, 128.00, 125.65, 125.08, 122.55, 120.98, 120.00, 55.28, 40.49, 31.78, 30.05, 29.23, 23.84, 22.60, 14.08. ($C_{61}H_{61}N_3$) (836): Calcd. C 87.56, H 7.30, N 5.02; Found C 87.37, H 7.41, N 5.05.

Other copolymers showed NMR and FT-IR spectra similar to that of PFTQ-50 copolymer except that the relative intensities of the signals are different due to the different composition of the copolymer.

3. Results and discussion

3.1. Synthesis and characterization

The synthetic procedures used to prepare the monomers and polymers are outlined in Fig. 1. A kind of improved Ullmann reaction [45] with the catalysts system consists of phenanthroline, CuCl and KOH is employed to synthesize the intermediate *N*,*N*-bis (4-bromophenyl)aniline (**1**). The preparation of compound **1** via the direct bromination of triphenylamine [46,47] is somewhat inconvenient due to the difficulty to distract the desired di-brominated triphenylamine from the crude product, which includes the byproducts of mono- and tri-brominated triphenylamines at the same time. The Ullmann reaction employed in our experiment is based on the higher reactivity of the iodo-group relative to that of the bromo-group, which can guarantee that the reaction only happens at the iodo-substituted site under this condition. The purification can be easily realized owing to the absence of disturbed mono- and tri-brominated byproducts. The compound **1** was successfully iodinated at the remaining *para*-site of the triphenylamine group with potassium iodide–potassium iodate in acetic acid [48–50] to afford the compound **2**. The compound **3** was prepared from the Sonogashira coupling [51] between the compound **2** and phenylacetylene. Its synthesis was also based on the much higher reactivity of iodo-group than that of bromo-group toward the Sonogashira coupling reaction. As a result, the iodo-substituted site was exclusively alkynylated by the controlling of feed ratio and reaction temperature. The triple bound in compound **3** can be oxidized to diketones at the presence of $KMnO_4$ [41], and the resulting oxidization product was directly condensed with 1,2-phenylenediamine in acetic acid to successfully afford the target monomer **4**.

Random and alternating PFTQ-series copolymers were synthesized by Suzuki coupling polymerization [44]. The molar ratios of the triphenylamine–quinoxaline moiety in the copolymers were controlled by adjusting the molar ratio between 9,9-dioctyl-2,7-dibromofluorene (**5**) and *N*,*N*-bis(4-bromophenyl)-4′-(3-phenylquinoxaline) phenylamine (**4**) while maintaining a 1:1 molar ratio between the dibromides and the bis(4,4,5,5-tetramethyl-1,3,2-dioxaborolan-2-yl). The comonomer feed ratios of the monomer **5** to the monomer **4** are 49:1, 45:5, 35:15, 20:30 and 0:50, and the corresponding copolymers are named as PFTQ-1, PFTQ-5, PFTQ-15, PFTQ-30 and PFTQ-50, respectively. The polyfluorene homopolymer (PFO) and the alternating copolymer of 2,7-fluorene and 4,4′-triphenylamine, poly(9,9-dioctylfluorene-*co*-4,4′-triphenylamine) (PFTPA), were also prepared using the same polymerization condition to make comparison. All of the copolymers are readily soluble in common organic solvents such as chloroform, toluene, and tetrahydrofuran (THF). The number-average molecular weights (M_n) of these polymers are determined by GPC against polystyrene standards to be 9000–18000, and with polydispersity indices of 1.65–2.30.

The chemical structures of all the intermediates and polymers are verified by NMR and FT-IR analyses. Fig. 2 shows the ^{1}H NMR spectra of the monomer **4** (Fig. 2a) and the representative alternating copolymer PFTQ-50 (Fig. 2b). One can see from Fig. 2a that two small signals appear at $\delta \sim 8.18$ and ~ 7.79 ppm, which can be assigned to the protons (labeled "a" and "b" in Fig. 2a) located at the quinoxaline unit. The multiple peaks in the range of 7.57–6.52 ppm correspond to the other aromatic protons in monomer **4**. As can be seen in Fig. 2b, a signal at $\delta \sim 8.23$ ppm (labeled "a" in Fig. 2b), which corresponds to the protons located at the quinoxaline unit and adjacent to the nitrogen atom, can also be observed in the ^{1}H NMR spectrum of PFTQ-50 as is found in the spectrum of the monomer **4** (Fig. 2a). This indicates that the triphenylamine–quinoxaline

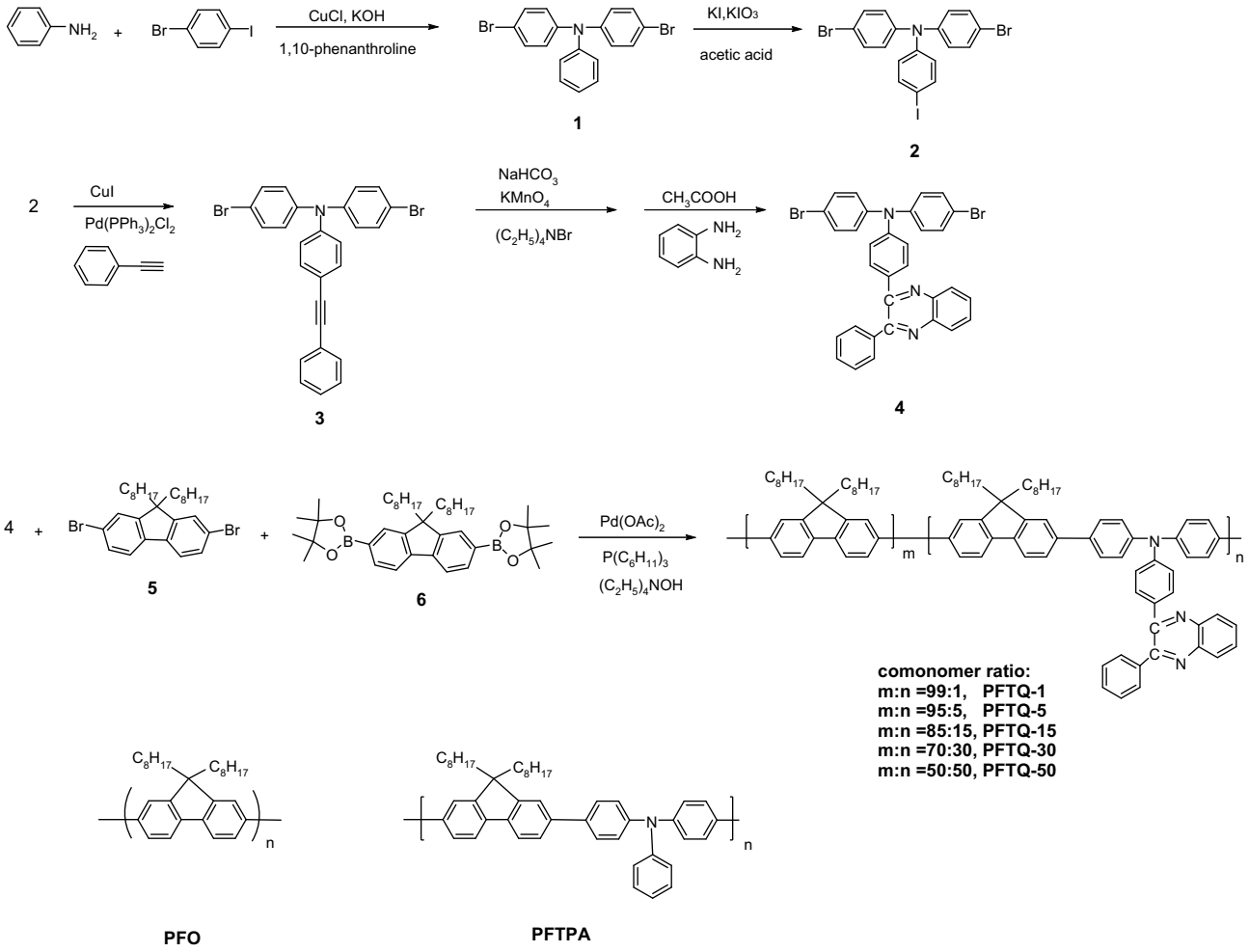

Fig. 1. Synthetic route of monomers and polymers (the chemical structures of the reference polymers are also showed here).

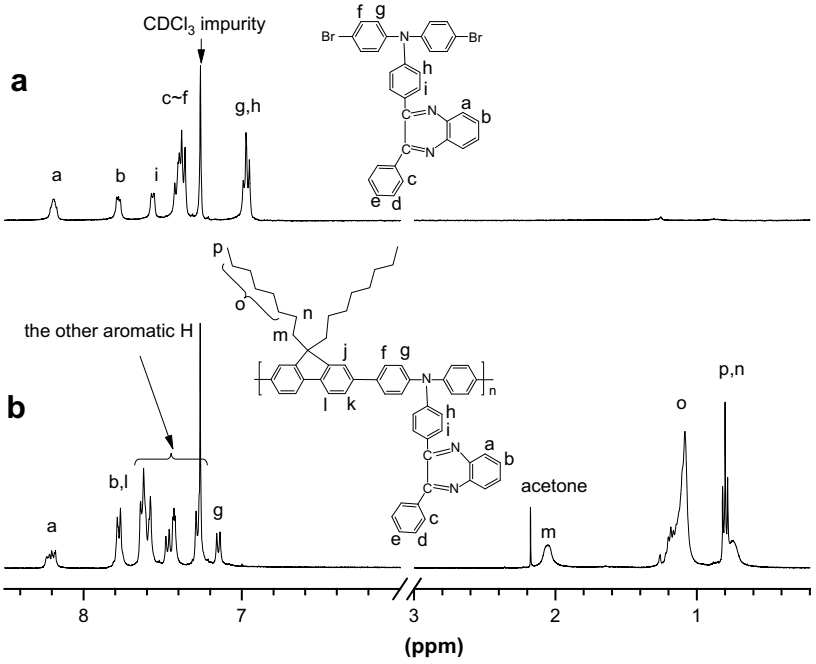

Fig. 2. ^{1}H NMR spectra of the monomer **4** (a) and PFTQ-50 copolymer (b) in $CDCl_3$.

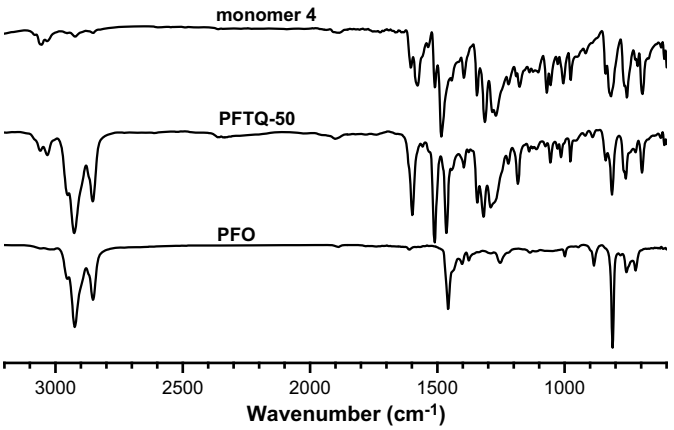

Fig. 3. FT-IR spectra of the monomer **4**, PFTQ-50 and PFO.

segment has been successfully introduced into the polymer after the polymerization reaction. The multiple peaks at the region of δ 7.79–7.14 ppm correspond to the other aromatic protons in PFTQ-50. The resonances at $\delta \sim$ 2.06, 1.16, and 0.82 ppm are assigned to the aliphatic protons in the octyl side chains. The molecular structures of intermediates and polymers are also reflected by their FT-IR spectra. FT-IR spectra of the monomer **4**, PFTQ-50 and the counterpart polymer PFO are shown in Fig. 3. Compared to the spectrum of PFO, the new vibrational bands at $\sim$ 1598 and $\sim$1510 cm^{-1} appear in the FT-IR spectra of monomer **4** and PFTQ-50, which are stem from the stretching vibrations of the C═N group in the quinoxaline ring [52].

The thermal properties of these copolymers are evaluated by TGA and DSC analyses, and the corresponding thermograms are depicted in Fig. 4. TGA revealed that the decomposition onset temperatures of these copolymers are ranging from 415 to 430 °C. Form the DSC curves of these polymers (the inset of Fig. 4) one can see that PFTQ-1 exhibited a glass transition process at around 155 °C. For the other four polymers containing the higher contents of triphenylamine–quinoxaline moieties, no distinct thermal transition was observed in the range of 30–200 °C. The chain motions in these polymers probably are restrained by the presence of the propeller-shaped triphenylamine in backbone and the bulky quinoxaline in pendant. TGA and DSC analyses suggest that these copolymers possess prominent thermal stability and can sufficiently meet the requirement for the application in flat panel displays.

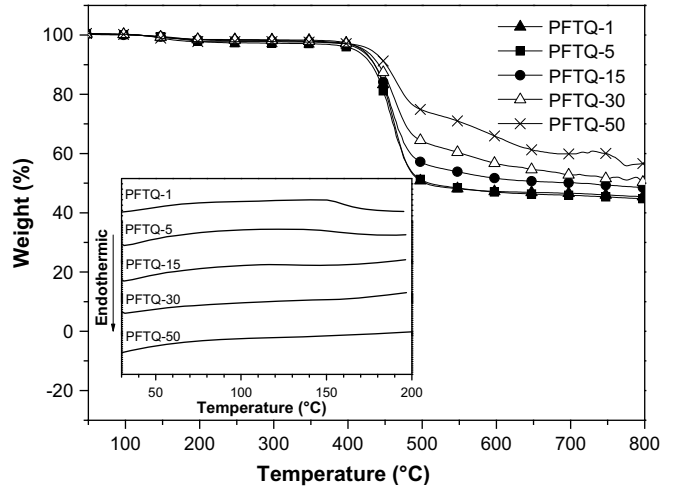

Fig. 4. TGA spectra of copolymers in nitrogen (the inset is the DSC curves of copolymers).

3.2. Optical properties of the polymers

The optical properties of these copolymers are measured both in solution and in thin films. Fig. 5 shows the UV–vis absorption spectra of these copolymers in toluene (Fig. 5a) ($\sim 1 \times 10^{-5}$ M based on the polymer repeat unit) and in solid films (Fig. 5b). The UV–vis spectra of PFO and PFTPA are also depicted here for comparison. As shown in Fig. 5a, the maximum absorptions of these copolymers are in the range of 386–392 nm. These absorption peaks, which approach to the maximum absorptions of PFO (392 nm) and PFTPA (382 nm), can be attributed to the electronic transition (π–π^*) along the conjugated backbones [52]. From Fig. 5a one can also see that the absorption spectra of these polymers in toluene became progressively broaden from PFTQ-1 to PFTQ-50, with the absorption onsets extended from 417 (for PFTQ-1) to 456 nm (for PFTQ-50). The absorptions of the films of these polymers (Fig. 5b) peak at the region of 386–392 nm, with the absorption onsets of 423–471 nm. The optical band gaps of these polymers can be estimated from their respective thin films' absorption edges using the equation of $1240/\lambda_{onset}$, which are in the range of 2.64–2.94 eV. One can see from Fig. 5 that for these copolymers no obvious absorption peak appears at the region of 400–500 nm, both in solution and in solid cases. Such distinctive absorption peaks have been frequently observed in the cases of triphenylamine/quinoxaline based D–$(A)_n$–D type oligomers [39–41], and can be assigned to

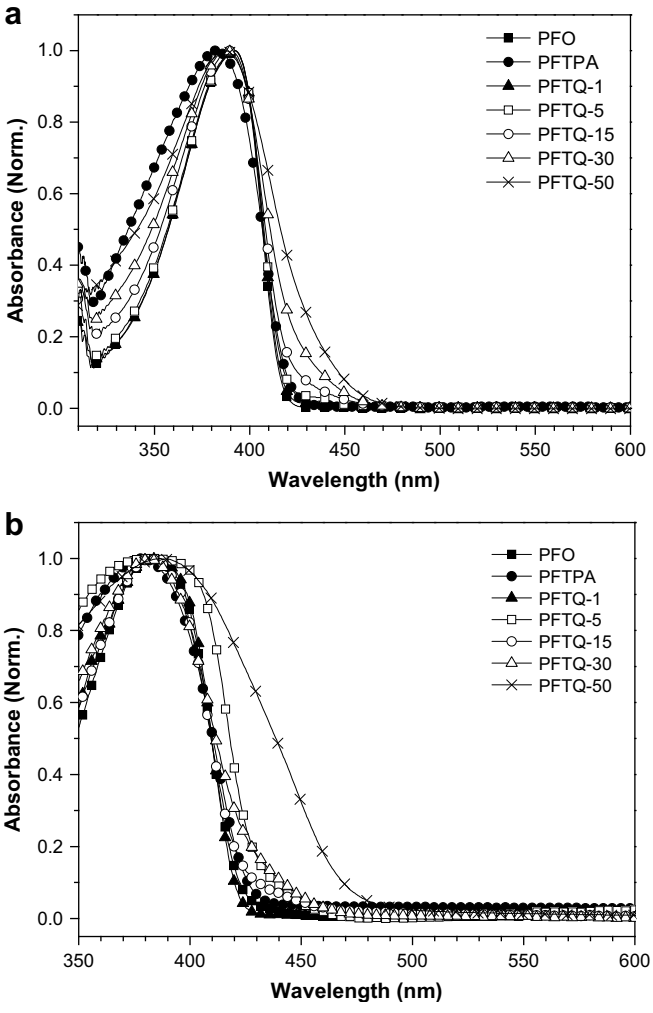

Fig. 5. UV–vis absorption spectra of polymers in toluene (a) and in films (b).

the strong ICT transition along the molecular chains between the electron-donating triphenylamine and the electron-accepting quinoxaline moieties [39–41]. The absence of the above-mentioned absorption peak in our case conveys that the ICT effect in these copolymers is not as strong as that of the D–$(A)_n$–D type oligomers due to the pendant-location of the electron-accepting quinoxaline group.

The PL emission spectra (excited by 360 nm) of PFTQ-series copolymers and the control polymers in toluene ($\sim 1 \times 10^{-5}$ M) are shown in Fig. 6a. The PL spectrum of PFO has the typical vibronic progression with the 0–0 emission band locate at 423 nm and the 0–1 transition at 440 nm [52], and the emission of PFTPA peaks at 441 nm. For PFTQ-1, the maximum emission appears at 423 nm and with a vibronic shoulder at 440 nm, accompanied by the appearance of a new broad emission band at the longer wavelength region (470–510 nm). As for PFTQ-5, two distinct emissions with the peak position separately at 423 and 496 nm can be observed. All of the other three copolymers with the higher composition ratio of D–A moiety (PFTQ-15, PFTQ-30 and PFTQ-50) exhibit the main emissions at ~ 498 nm and the emission bands at ~ 423 nm almost completely vanish. It indicates that the efficient energy-transfer happens between the fluorene segment (with the higher energy) and D–A moiety (with the lower energy).

The PL spectra of the films of PFTQ-series copolymers and the control polymers under the excitation of 360 nm are illustrated in Fig. 6b. The maximum emissions of PFO and PFTPA are at 435 nm and 440 nm, respectively. For PFTQ-series copolymers, their PL spectra display significant red-shift relative to that of PFO and PFTPA, and exhibit the emission peaks in the range of 475–510 nm. The emission spectra of them positively shift with the increase of the composition ratio of D–A segment. For these polymers the blue emission of fluorene segment in polymers' backbones are efficiently quenched by the D–A segments, even when the composition ratio of D–A moiety is just 1% in the case of PFTQ-1. The absolute PL quantum yields (Φ) of these polymers in the solid state, measured by using a calibrated integrating sphere, are in the range of 11.9–15.5%. The synthesis results, optical and thermal properties of these copolymers are summarized in Table 1. From Fig. 6 and Table 1 one can find that the PL emission maxima of these copolymers is close to those of the D–$(A)_n$–D type oligomers, both in dilute toluene solution and in solid state cases [40,41]. This finding indicates that the PL emission of these polymers still originates from their ICT excited states [40,41], in spite of the relatively weaker ICT in these polymers as compared to that of the D–$(A)_n$–D type oligomers.

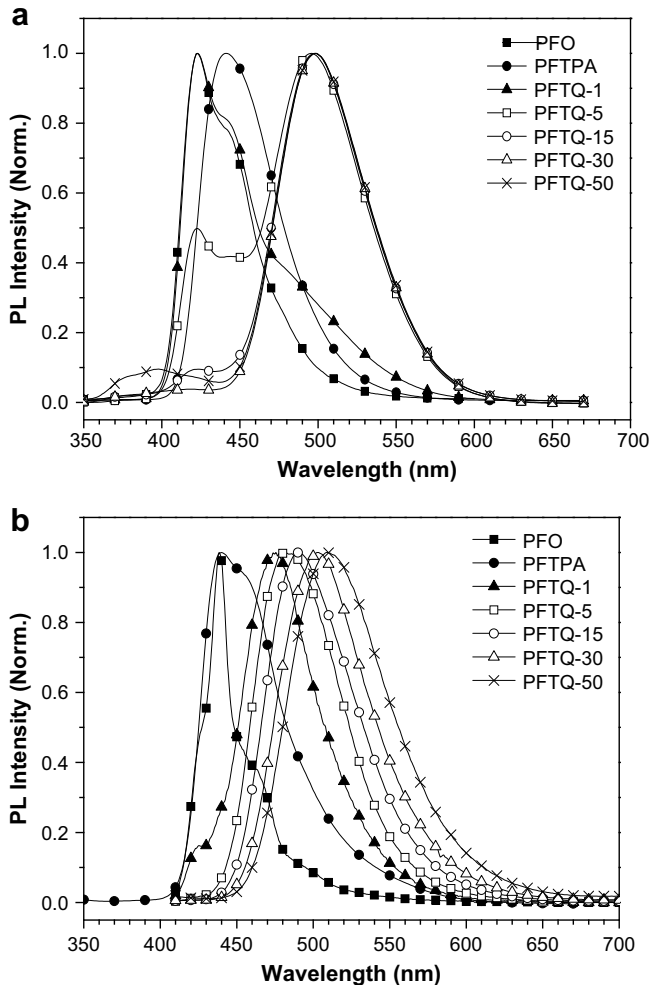

Fig. 6. PL emission spectra of polymers in toluene (a) and in films (b) (the excitation wavelength was 360 nm in both cases).

Table 1
Synthesis results, optical data and thermal properties of the copolymers.

Polymer	Yield (%)	M_n[a]	M_w/M_n	λ_{max} (nm; UV–vis)		λ_{EM}[b] (nm; FL)		T_d[c] (°C)	Φ[d] (%)
				In toluene	In films	In toluene	In films		
PFTQ-1	80	18,000	1.71	392	392	423	475	415	14.8
PFTQ-5	79	14,000	1.65	392	392	496	482	411	15.5
PFTQ-15	77	15,000	1.68	390	390	498	490	417	13.4
PFTQ-30	73	12,000	1.86	388	388	498	503	427	11.5
PFTQ-50	71	9,000	2.30	386	386	499	509	430	11.9

[a] Determined by GPC (with polystyrene standards).
[b] Position of the emission peak from PL data.
[c] The decomposition onset temperature obtained by TGA.
[d] Absolute quantum yield of the polymer films, measured by using a calibrated integrating sphere at an exciting wavelength of 325 nm.

3.3. Electrochemical properties

The electrochemical behaviors of these copolymers are investigated by cyclic voltammetry (CV). The electrochemical properties of these polymers in solid films are summarized in Table 2, and their CV curves are exhibited in Fig. 7. As can be seen from Fig. 7, all of these polymers afford highly reversible p-doping processes. The entire CV profiles of PFTQ-1 and PFTQ-5 are highly resemble to that of PFO due to the relatively lower D–A composition in their structures, and the oxidation onsets of both two polymers appeared at ~ 1.38 V. The oxidation onsets of the other three polymers gradually decreased accompanied by the increase of D–A composition, rang from 1.30 V for PFTQ-15 to 0.98 V for PFTQ-50, which stems from the increase of the electron-donating triphenylamine moieties' ratios in polymers' backbones, suggesting the modified hole-transport capability with the introduction of triphenylamine group. The energy levels of the highest occupied molecular orbital

Table 2
Electrochemical properties of copolymers.

Polymers	Optical band gap[a] (eV)	E_{ox} (V)	E_{HOMO} (eV)	E_{LUMO}[b] (eV)
PFTQ-1	2.94	1.38	−5.78	−2.84
PFTQ-5	2.83	1.38	−5.78	−2.95
PFTQ-15	2.86	1.30	−5.70	−2.84
PFTQ-30	2.72	1.15	−5.55	−2.83
PFTQ-50	2.64	0.98	−5.38	−2.74

[a] Estimated from the onset wavelength of optical absorption in the solid state film.
[b] Calculated from the HOMO level and optical band gap.

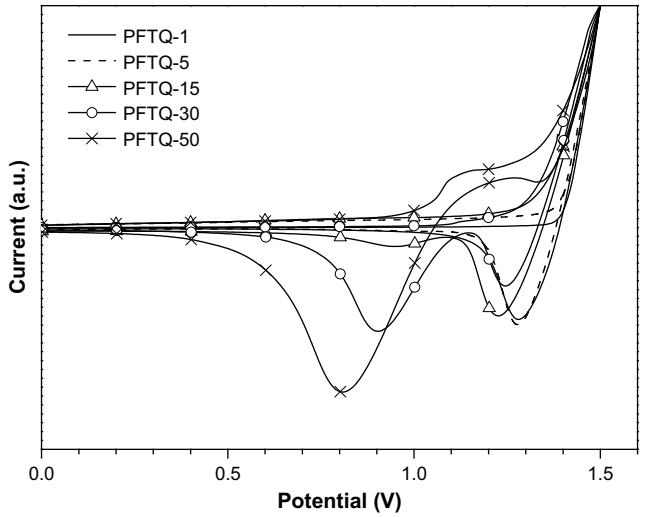

Fig. 7. Cyclic voltammograms of the polymers' films coated on platinum electrodes in 0.1 mol/L Bu_4NPF_6, CH_3CN solution.

(HOMO) of these copolymers can be estimated from the onsets of their oxidation waves, calculated according to an empirical formula, $E_{HOMO} = -e(E_{ox} + 4.4)$ (eV) [53], to be in the range of −5.38 to −5.78 eV. In the cathodic scan, unfortunately, no obvious reduction peak (down to −2.0 V *vs.* SCE) is observed for these copolymers. The levels of the lowest unoccupied molecular orbital (LUMO) of them can be estimated by subtracting their optical band gaps from the corresponding HOMOs, are in the range of −2.74 to −2.95 eV. The HOMO level of the polymer PFTQ-50 (−5.38 eV) is very close to that of the triphenylamine–quinoxaline based oligomers due to the identical oxidation site, the electron-donating triphenylamine they possess [39–41]. On the other hand, the LUMO level of PFTQ-50 (−2.74 eV) is slightly higher than that of the triphenylamine–$(quinoxaline)_2$–tripenylamine type oligomers (−2.92 eV) [41] and lower than that of the triphenylamine–$(quinoxaline)_1$–tripenylamine type oligomers (−2.57 eV) [40]. Considering the same donor (triphenylamine) and acceptor (quinoxaline) moieties involved in these oligomers and PFTQ-50, the difference between the LUMO levels of them was presumably brought by the different composition ratios of donor/acceptor moieties in these materials, i.e., the LUMO levels gradually decreased with the increase of the composition of electron-accepting moieties.

3.4. Electroluminescence properties

Non-optimized devices with the structure of ITO/PEDOT:PSS/emissive polymer/Ba/Al were fabricated to investigate the electroluminescence properties of these polymers. The corresponding control devices with PFO and PFTPA as emissive layers (EMLs) were simultaneously fabricated for comparison. The detailed performance data are listed in Table 3. Fig. 8 shows the normalized EL spectra of above-mentioned devices. As shown in Fig. 8, the EL spectra of these copolymers are almost indistinguishable from their corresponding thin films' PL spectra, suggesting the same emission site for both cases. The EL emission of these copolymers is close to that of the triphenylamine/quinoxaline based D–$(A)_n$–D type oligomers [40,41], which is consistent with the finding in their PL cases. Fig. 9 depicts the current density–voltage (Fig. 9a), the brightness–voltage (Fig. 9b) and the external quantum efficiency–current density (Fig. 9c) relationships of these devices. Form Table 3 and Fig. 9 one can note that the devices' performance is considerably improved after the introduction of the D–A segment into polymers as compared with that of the control devices. All of the PFTQ-series

Table 3
Characteristics of the devices with the structure of ITO/PEDOT:PSS/polymer/Ba/Al.

Polymers	Device performances				
	Turn-on voltage[a] (V)	Max Lumin. (cd m^{-2}) (Bias (V))	Max QE (%) (Bias(V))	λ_{max}[b] (nm)	CIE 1931[c] (*x*,*y*)
PFO	4.0	1228 (6.2)	0.30 (5.0)	440	(0.19, 0.19)
PFTPA	4.2	48 (6.2)	0.009 (6.0)	430	(0.19, 0.14)
PFTQ-1	5.0	1911(8.2)	1.22 (7.5)	478	(0.18, 0.31)
PFTQ-5	5.5	3926 (9.5)	1.74 (8.5)	484	(0.19, 0.40)
PFTQ-15	6.2	2098 (10.5)	1.06 (8.7)	494	(0.22, 0.47)
PFTQ-30	5.5	3198 (8.7)	0.62 (7.7)	500	(0.21, 0.50)
PFTQ-50	4.0	2568 (7.0)	0.73 (5.5)	504	(0.24, 0.49)

[a] Voltage required for a device to reach the luminescence of ~1 cd/m^2.
[b] Position of emission peak from EL data.
[c] The CIE coordinates are calculated at the maximum EQE.

polymers based devices give the higher maximum brightness and QE than that of the control devices. The PFO and PFTPA based control devices exhibit the maximum brightness of 1228 cd/m^2 (6.25 V, 667 mA/cm^2) and 48 cd/m^2 (6.25 V, 637 mA/cm^2), and with the maximum QE of 0.3% (5.0 V, 566 mA/cm^2, 283 cd/m^2) and 0.009% (6.0 V, 516 mA/cm^2, 39 cd/m^2), respectively. The best performance among the PFTQ-series polymers based devices is achieved by PFTQ-5, which exhibit the maximum brightness of 3926 cd/m^2 (9.5 V, 273 mA/cm^2) and the maximum QE of 1.7% (8.5 V, 103 mA/cm^2, 1989 cd/m^2). The significantly enhanced device performance is clearly stem from the more balanced injection rates of both carriers due to the simultaneous introduction of triphenylamine and quinoxaline groups into these polymers. The devices based on copolymers with D–A fraction greater than 15 mol% exhibit relatively poorer performances, which is consistent with the finding in the characterization of a series of quinoxaline-containing polyfluorenes in previous report [52]. This reflects the importance of the composition of polymers' structures to the modulation of their EL performance. As a whole, the EL performances of these copolymers are comparable or slightly inferior to that of the triphenylamine/quinoxaline based D–$(A)_n$–D type oligomers [39–41], even with the much simpler devices' configurations at this stage. According to the reports about these D–$(A)_n$–D type oligomers, their EL performances were substantially benefited from

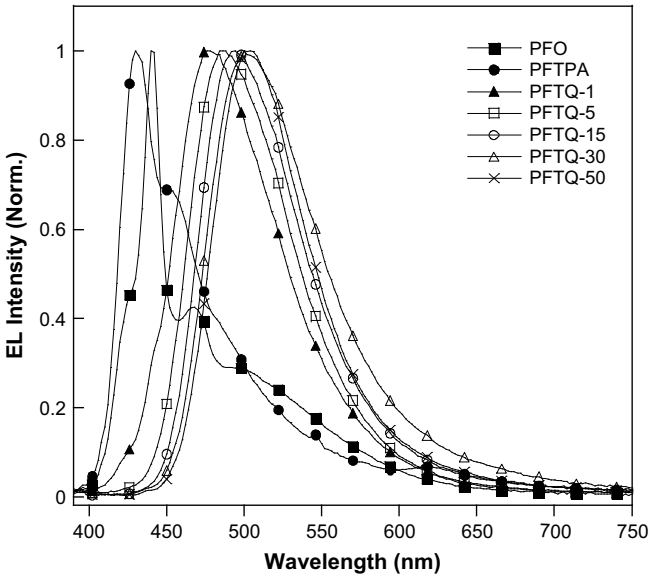

Fig. 8. Normalized EL spectra of the devices.

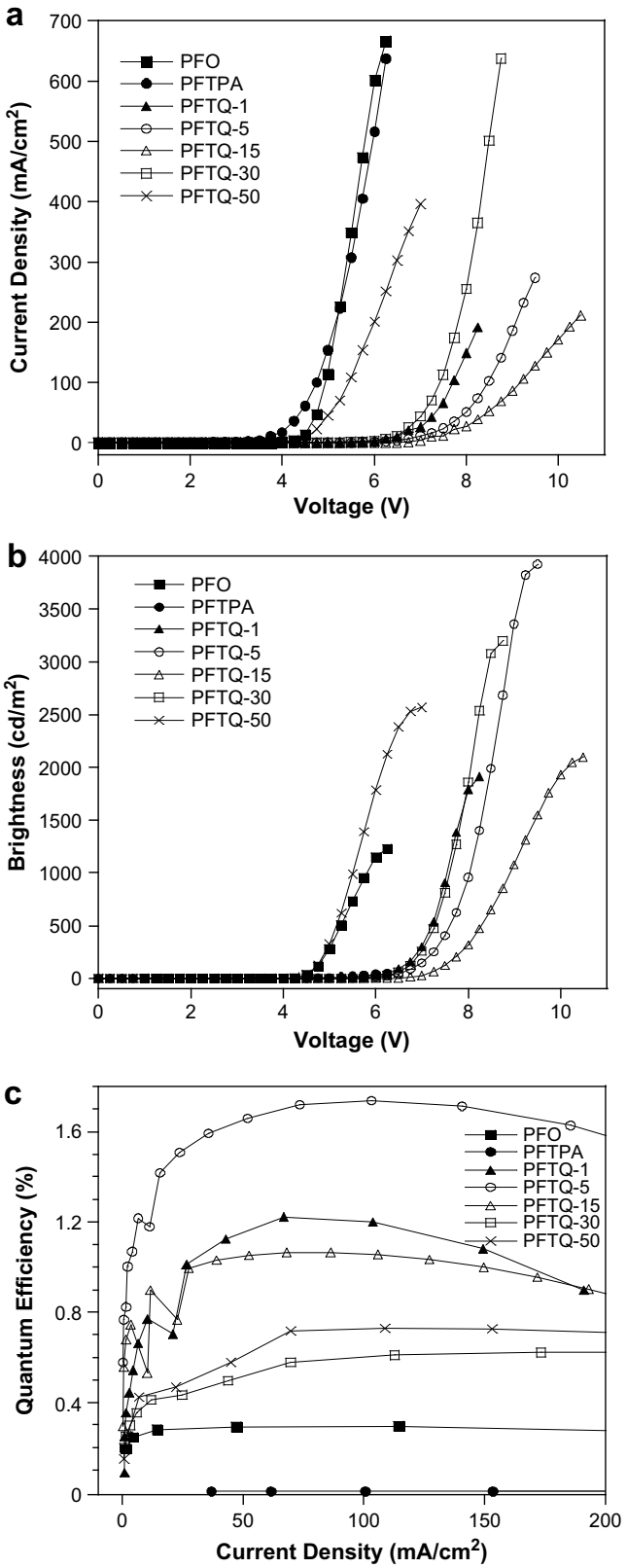

Fig. 9. The current density–voltage (a), brightness–voltage (b) and external quantum efficiency–current density (c) relationships of the devices.

the introduction of the electron and hole-blocking layers [39–41]. Considering that no additional electron and hole-blocking layer was employed in the current investigation, we believe that there are still some enhancement spaces for the EL performance of such PFTQ-series polymers with further devices' optimization.

4. Conclusions

We have synthesized a series of novel polyfluorene derivatives, which containing the electron-donating triphenylamine group in polymers' backbone and the electron-withdrawing quinoxaline in pendant through Suzuki coupling reaction. These copolymers exhibited excellent solubility in common organic solvents, good processability and high thermal stability. Devices based on these copolymers showed superior electroluminescent performance relative to that of the PFO and PFTPA based control devices. Such polymers represent a new set of potential emissive materials in the application of PLEDs.

Acknowledgments

The authors greatly appreciate the financial support from the National Natural Science Foundation of China (Project No. 20674066), the Natural Science Foundation of Xinjiang Uygur Autonomous Region (Project No. 200821123) and the Scientific Research Starting Foundation for Doctoral Graduate, Xinjiang University (Grant No. BS080110). We greatly thank Prof. Yong Cao (Institute of Polymer Optoelectronic Materials and Device, Key Lab of Specially Functional Materials of the Ministry of Education, South China University of Technology) for his help in the measurement of electroluminescent devices.

References

[1] Kraft A, Grimsdale AC, Holmes AB. Electroluminescent conjugated polymers – seeing polymers in a new light. Angewandte Chemie International Edition 1998;37(4):402–28.
[2] Friend RH, Gymer RW, Holmes AB, Burroughes JH, Marks RN, Taliani C, et al. Electroluminescence in conjugated polymers. Nature 1999;397(14):121–8.
[3] Rees ID, Robinson KL, Holmes AB, Towns CR, O'Dell R. Recent developments in light-emitting polymers. MRS Bulletin 2002;27(6):451–5.
[4] Heeger AJ. Light emission from semiconducting polymers: light-emitting diodes, light-emitting electrochemical cells, lasers and white light for the future. Solid State Communications 1998;107(11):673–9.
[5] Sheats JR, Antoniadis H, Hueschen M, Leonard W, Miller J, Moon R, et al. Organic electroluminescent devices. Science 1996;273(5277):884–8.
[6] Tarkka RM, Zhang X, Jenekhe SA. Electrically generated intramolecular proton transfer: electroluminescence and stimulated emission from polymers. Journal of the American Chemical Society 1996;118(39):9438–9.
[7] Jenekhe SA, Zhang X, Chen XL, Choong VE, Gao Y, Hsieh BR. Finite size effects on electroluminescence of nanoscale semiconducting polymer heterojunctions. Chemistry of Materials 1997;9(2):409–12.
[8] Zhang X, Jenekhe SA. Electroluminescence of multicomponent conjugated polymers 1. Roles of polymer/polymer interfaces in emission enhancement and voltage-tunable multicolor emission in semiconducting polymer/polymer heterojunctions. Macromolecules 2000;33(6):2069–82.
[9] Tonzola CJ, Alam MM, Jenekhe SA. New soluble n-type conjugated copolymer for light-emitting diodes. Advanced Materials 2002;14(15):1086–90.
[10] Gustafsson G, Cao Y, Treacy GM, Klavetter F, Colaneri N, Heeger AJ. Flexible light-emitting diodes made from soluble conducting polymers. Nature 1992;357:477–9.
[11] Greenham NC, Moratti SC, Bradley DDC, Friend RH, Holmes AB. Efficient light-emitting diodes based on polymers with high electron affinities. Nature 1993;365:628–30.
[12] Zhu Y, Alam MM, Jenekhe SA. Regioregular head-to-tail poly(4-alkylquinoline)s: synthesis, characterization, self-organization, photophysics, and electroluminescence of new n-type conjugated polymers. Macromolecules 2003;36(24):8958–68.
[13] Tonzola CJ, Alam MM, Kaminsky W, Jenekhe SA. New n-type organic semiconductors: synthesis, single crystal structures, cyclic voltammetry, photophysics, electron transport, and electroluminescence of a series of diphenylanthrazolines. Journal of the American Chemical Society 2003;125(44):13548–58.

[14] Alam MM, Jenekhe SA. Polybenzobisazoles are efficient electron transport materials for improving the performance and stability of polymer light-emitting diodes. Chemistry of Materials 2002;14(11):4775–80.
[15] Chen BZ, Wu YZ, Wang MZ, Wang S, Sheng SH, Zhu WH, et al. Novel fluorene-alt-thienylenevinylene-based copolymers: tuning luminescent wavelength via thiophene substitution position. European Polymer Journal 2004;40(6):1183–91.
[16] Strukelj M, Papadimitrakopoulos F, Miller TM, Rothberg LJ. Design and application of electron-transporting organic materials. Science 1995;267(5206):1969–72.
[17] Jenekhe SA, Lu L, Alam MM. New conjugated polymers with donor–acceptor architectures: synthesis and photophysics of carbazole–quinoline and phenothiazine–quinoline copolymers and oligomers exhibiting large intramolecular charge transfer. Macromolecules 2001;34(21):7315–24.
[18] Champion RD, Cheng KF, Pai CL, Chen WC, Jenekhe SA. Electronic properties and field-effect transistors of thiophene-based donor–acceptor conjugated copolymers. Macromolecular Rapid Communications 2005;26(23):1835–40.
[19] Yamamoto T, Yasuda T, Sakai Y, Aramaki S. Ambipolar field-effect transistor (FET) and redox characteristics of a π-conjugated thiophene/1,3,4-thiadiazole CT-type copolymer. Macromolecular Rapid Communications 2005;26(15):1214–7.
[20] Kulkarni AP, Tonzola CJ, Babel A, Jenekhe SA. Electron transport materials for organic light-emitting diodes. Chemistry of Materials 2004;16(23):4556–73.
[21] Bao Z, Peng ZH, Galvin ME, Chandross EA. Novel oxadiazole side chain conjugated polymers as single-layer light-emitting diodes with improved quantum efficiencies. Chemistry of Materials 1998;10(5):1201–4.
[22] Lee YZ, Chen X, Chen SA, Wei PK, Fann WS. Soluble electroluminescent poly(phenylenevinylene)s with balanced electron- and hole injections. Journal of the American Chemical Society 2001;123(10):2296–307.
[23] Kim JH, Park JH, Lee H. Highly efficient novel poly(*p*-phenylenevinylene) derivative with 1,3,4-oxadiazole pendant on a vinylene unit. Chemistry of Materials 2003;15(18):3414–6.
[24] Tang CW, VanSlyke SA, Chen CH. Electroluminescence of doped organic thin films. Journal of Applied Physics 1989;65(9):3610–6.
[25] Adachi C, Tsutsui T, Saito S. Organic electroluminescent device having a hole conductor as an emitting layer. Applied Physics Letters 1989;55(15):1489–91.
[26] VanSlyke SA, Chen CH, Tang CW. Organic electroluminescent devices with improved stability. Applied Physics Letters 1996;69(15):2160–2.
[27] Nomura M, Shibasaki Y, Ueda M, Tugita K, Ichikawa M, Taniguchi Y. Synthesis and properties of poly[di(1-naphthyl)-4-tolylamine] as a hole transport material. Macromolecules 2004;37(4):1204–10.
[28] Yu WL, Pei J, Huang W, Heeger AJ. A novel triarylamine-based conjugated polymer and its unusual light-emitting properties. Chemical Communications 2000:681–2.
[29] Jung BJ, Lee JI, Chu HY, Do LM, Shim HK. Synthesis of novel fluorene-based poly(iminoarylene)s and their application to buffer layer in organic light-emitting diodes. Macromolecules 2002;35(6):2282–7.
[30] Shi W, Fan SQ, Huang F, Yang W, Liu RS, Cao Y. Synthesis of novel triphenylamine-based conjugated polyelectrolytes and their application as hole-transport layers in polymeric light-emitting diodes. Journal of Materials Chemistry 2006;16:2387–94.
[31] Xiao HB, Leng B, Tian H. Hole transport triphenylamine–spirosilabifluorene alternating copolymer: synthesis and optical, electrochemical and electroluminescent properties. Polymer 2005;46(15):5707–13.
[32] Thelakkat M, Hagen J, Haarer D, Schmidt HW. Poly(triarylamine)s-synthesis and application in electroluminescent devices and photovoltaics. Synthetic Metals 1999;102:1125–8.
[33] Zhan XW, Liu YQ, Wu X, Wang S, Zhu DB. New series of blue-emitting and electron-transporting copolymers based on fluorene. Macromolecules 2002;35(7):2529–37.
[34] Sun QJ, Zhan XW, Yang CH, Liu YQ, Zhu DB. Photo- and electroluminescence properties of fluorene-based copolymers containing electron- or hole-transporting unit. Thin Solid Films 2003;440(1-2):247–54.
[35] Nurulla I, Yamaguchi I, Yamamoto T. Preparation and properties of new π-conjugated polyquinoxalines with aromatic fused rings in the side chain. Polymer Bulletin 2000;44:231–8.
[36] O'Brien D, Weaver MS, Lidzey DG, Bradley DDC. Use of poly(phenyl quinoxaline) as an electron transport material in polymer light-emitting diodes. Applied Physics Letters 1996;69(7):881–3.
[37] Fukuda T, Kanbara T, Yamamoto T, Ishikawa K, Takezoe H, Fukuda A. Polyquinoxaline as an excellent electron injecting material for electroluminescent device. Applied Physics Letters 1996;68(17):2346–8.
[38] Cui YT, Zhang XJ, Jenekhe SA. Thiophene-linked polyphenylquinoxaline: a new electron transport conjugated polymer for electroluminescent devices. Macromolecules 1999;32(11):3824–6.
[39] Chen SY, Xu XJ, Liu YQ, Yu G, Sun XB, Qiu WF, et al. Synthesis and characterization of n-type materials for non-doped organic red-light-emitting diodes. Advanced Functional Materials 2005;15(9):1541–6.
[40] Chen SY, Xu XJ, Liu YQ, Qiu WF, Yu G, Wang HP, Zhu DB. New organic light-emitting materials: synthesis, thermal, photophysical, electrochemical, and electroluminescent properties. The Journal of Physical Chemistry C 2007;111(2):1029–34.
[41] Hancock JM, Gifford AP, Zhu Y, Lou Y, Jenekhe SA. *n*-Type conjugated oligoquinoline and oligoquinoxaline with triphenylamine endgroups: efficient ambipolar light emitters for device applications. Chemistry of Materials 2006;18(20):4924–32.
[42] Hou Q, Xu YS, Yang W, Yuan M, Peng JB, Cao Y. Novel red-emitting fluorene-based copolymers. Journal of Materials Chemistry 2002;12:2887–92.
[43] Yang RQ, Tian RY, Yang W, Hou Q, Cao Y. Synthesis and optical and electroluminescent properties of novel conjugated copolymers derived from fluorene and benzoselenadiazole. Macromolecules 2003;36(20):7453–60.
[44] Wang EG, Li C, Mo YQ, Zhang Y, Ma G, Shi W, et al. Poly(3,6-silafluorene-co-2,7-fluorene)-based high-efficiency and color-pure blue light-emitting polymers with extremely narrow band-width and high spectral stability. Journal of Materials Chemistry 2006;16:4133–40.
[45] Goodbrand HB, Hu NX. Ligand-accelerated catalysis of the Ullmann condensation: application to hole conducting triarylamines. The Journal of Organic Chemistry 1999;64(2):670–4.
[46] Kim SW, Shim SC, Kim DY, Kim CY. Synthesis and properties of novel triphenylamine polymers containing ethynyl and aromatic moieties. Synthetic Metals 2001;122(2):363–8.
[47] Lee HJ, Sohn J, Hwang J, Park SY, Choi H, CHa M. Triphenylamine-cored bifunctional organic molecules for two-photon absorption and photorefraction. Chemistry of Materials 2004;16(3):456–65.
[48] Sonntag M, Kreger K, Hanft D, Strohriegl P, Setayesh S, Leeuw DD. Novel star-shaped triphenylamine-based molecular glasses and their use in OFETs. Chemistry of Materials 2005;17(11):3031–9.
[49] Hohle C, Hofmann U, Schloter S, Thelakkat M, Strohriegl P, Haarer D, et al. Photorefractive triphenylamine-based glass: a multifunctional low molecular weight compound with fast holographic response. Journal of Materials Chemistry 1999;9:2205–10.
[50] Ning ZJ, Chen Z, Zhang Q, Yan YL, Qian SX, Cao Y, et al. Aggregation-induced emission (AIE)-active starburst triarylamine fluorophores as potential non-doped red emitters for organic light-emitting diodes and Cl2 gas chemodosimeter. Advanced Functional Materials 2007;17(18):3799–807.
[51] Sonogashira K, Tohda Y, Hagihara N. A convenient synthesis of acetylenes: catalytic substitutions of acetylenic hydrogen with bromoalkenes, iodoarenes and bromopyridines. Tetrahedron Letters 1975;16(50):4467–70.
[52] Kulkarni AP, Zhu Y, Jenekhe SA. Quinoxaline-containing polyfluorenes: synthesis, photophysics, and stable blue electroluminescence. Macromolecules 2005;38(5):1553–63.
[53] Leeuw DM, Simenon MMJ, Brown AR, Einerhand REF. Stability of n-type doped conducting polymers and consequences for polymeric microelectronic devices. Synthetic Metals 1997;87(1):53–9.